Analysis of Compact E-Plane Diplexers in Rectangular Waveguide

Antonio Morini, *Member, IEEE*, and Tullio Rozzi, *Fellow, IEEE*

***Abstract*—Photolithographic techniques permit the realization of complex circuits totally confined to the E-plane of millimetric rectangular guides with high precision and low cost. This work contains a detailed analysis of an E-plane diplexer configuration recently introduced. Its main feature is the matching section of the three port junction, a simple abrupt E-plane one tuned by means of an inductive post realized on the same mask as the branching filters. On the basis of this analysis, we also demonstrate the application of a recently developed diplexer synthesis technique. Many prototypes, in K_a-band were designed and tested, showing good performances and good agreement between theory and experiment.**

I. Introduction

IN REALIZING millimetric diplexers, it is increasingly expedient both technically and economically to employ reciprocal circuits instead of the traditional microwave circulators [1]–[5]. This is why we recently proposed an E-plane diplexer configuration [6] that is based on the abrupt three-port junction, in lieu of a tapered junction [2]–[4] requiring more expensive mechanical construction. The junction is tuned by means of a single inductive post built on the same mask as the E-plane filters, and placed between the junction and the bifurcation, as shown in Fig. 1. The resulting diplexer consists of just three parts: a single mask containing filters and tuning post and the two halves of the housing wherefrom junction and guides are made. The diplexer is assembled by sandwiching the mask [Fig. 2(b)] between the two halves of the housing [Fig. 2(a)]. Modeling the junction, inclusive of the post, involves a rigorous treatment of the interaction between adjacent discontinuities by the concept of accessible modes [7].

As contrasted to [7], modes of both TE and TM polarization occur depending on two indices with corresponding additional complexity of the analysis.

We now provide a full analytical model for this kind of configuration, that can be coded for running on a PC without recourse to field analysis.

We also demonstrate the utilization of this analysis to the synthesis of various K_a-band prototypes that were actually built and tested, showing good performances and good agreement with predictions.

For the sake of readability of the main text, details of the calculations are reported in Appendix.

Manuscript received June 20, 1994; revised April 24, 1995.

The authors are with the Dipartimento di Elettronica ed Automatica Università di Ancona, 60100 Ancona, Italy.

IEEE Log Number 9412689.

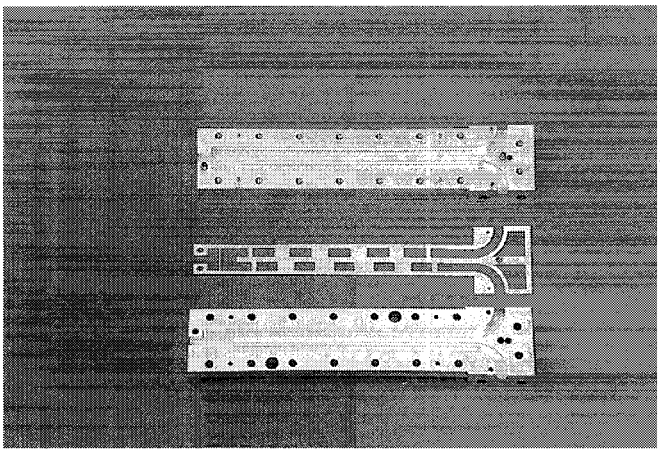

Fig. 1. Compact E-plane diplexer.

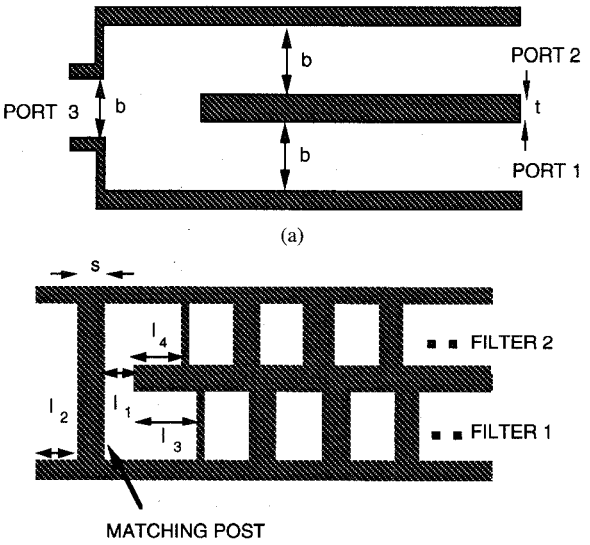

Fig. 2. (a) E-plane section of the three-port junction. (b) Mask containing filters and matching posts.

II. Diplexer Analysis

We shall now focus on the analysis of the junction, whereas reference is made to [7] for that of the filters. Symmetry of the three-port junction about its longitudinal mid-plane [Fig. 2(a)] implies $s_{11} = s_{22}$ e $s_{13} = s_{23}$, so that its scattering matrix becomes

$$\begin{bmatrix} b_1 \\ b_2 \\ b_3 \end{bmatrix} = \begin{bmatrix} s_{11} & s_{12} & s_{13} \\ s_{12} & s_{11} & s_{13} \\ s_{13} & s_{13} & s_{33} \end{bmatrix} \begin{bmatrix} a_1 \\ a_2 \\ a_3 \end{bmatrix}. \quad (1)$$

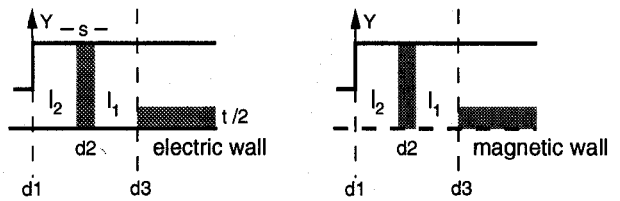

Fig. 3. Even/odd excitation at ports 1 and 2: Resulting structures.

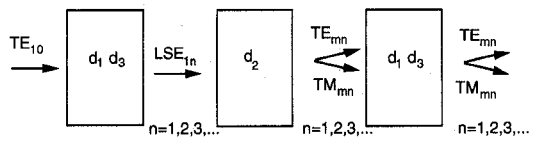

Fig. 4. Scheme of the modal interactions occurring between discontinuities.

By setting separately $a_1 = a_2 = 1$ $a_3 = 0$ and $a_1 = -a_2 = 1$ $a_3 = 0$, corresponding to the even and odd excitation, respectively, at ports 1 and 2, it is possible to characterize the junction. By substituting those values in (1), we obtain, in the even case

$$b_1^e = s_{11} + s_{12} \tag{2a}$$

$$b_3^e = 2s_{13} \tag{2b}$$

and, in the odd case

$$b_1^o = s_{11} - s_{12}. \tag{2c}$$

The parameter s_{33} is recovered by the losslessness condition

$$s_{13}s_{11}^* + s_{13}s_{12}^* + s_{33}s_{13}^* = 0 \tag{2d}$$

which gives

$$s_{33} = -\frac{s_{13}s_{11}^* + s_{13}s_{12}^*}{s_{13}^*}. \tag{2e}$$

Note also that this latter condition implies $|s_{33}| = |b_1^e|$.

By applying even and odd excitations, the three-port junction reduces to the two two-port situations shown in Fig. 3; both comprise the cascade of three discontinuities $d1$, $d2$, and $d3$ separated by short sections of guide and, as such, interacting. These discontinuities are analyzed individually as $2N$-port, N being the number of $'$ accessible modes $'$ chosen according to the following considerations.

Owing to their uniformity with respect to x, discontinuities 1 and 3, that is the two E-plane steps, under the excitation of an incident TE_{10}-mode excite in turn just LSE_{1n}-modes with $n = 1, 2, 3 \cdots$.

On the other hand, due to its uniformity with respect to y, discontinuity 2, i.e., the metal septum, when excited by LSE_{1n}-modes excites in turn the TE_{mn} and TM_{mn} families with $m = 1, 3, 5 \cdots$. Finally, the latter impinging on discontinuities 1 and 3 excite TE_{mn} and TM_{mn} modes with $n = 1, 2, 3 \cdots$.

This complex mechanism is summarized in Fig. 4.

For this reason, we preferred to work with the TE and TM families, rather than LSE, LSM for both types of discontinuities. Modes with attenuation larger than 20 dB between successive discontinuities were considered "localized." In order to understand what this assumption implies, consider that for $b \leq \frac{3}{2}a$, the attenuation of the first mode below-cutoff that is being excited, i.e., TE_{13}, is greater than 40 dB/λ_g. In this case, it is sufficient to consider TE_{10}, TE_{11}, TM_{11}, TE_{12}, and TM_{12} as accessible modes obtaining accurate results for discontinuities spaced at least $\lambda_g/2$.

Moreover, it has to be noted that the present approach avoids any numerical instability of the kind discussed in [8]. In fact, the interaction between cascaded discontinuities is accounted for just by those modes that are actually significant and numerical instability due to the weak interactions by higher order modes is thereby avoided.

In practice, once the diplexer is designed on the basis of the five modes model, we have to check its dimensions in order to verify the consistency of the model itself.

If the result is negative, for instance the attenuation of the lowest "localized" mode [9] is less than 20 dB at the upperband edge, we include that mode among the accessible ones.

Each of the six discontinuities occurring is analyzed by deriving a rigorous variational expression of its multiport impedance matrix of the type

$$\begin{bmatrix} \mathbf{V}_{e/o}^l \\ \mathbf{V}_{e/o}^r \end{bmatrix} = \begin{bmatrix} \mathbf{z}_{e/o}^{ll} & \mathbf{z}_{e/o}^{lr} \\ \mathbf{z}_{e/o}^{rl} & \mathbf{z}_{e/o}^{ll} \end{bmatrix}^{(k)} \begin{bmatrix} \mathbf{I}_{e/o}^l \\ \mathbf{I}_{e/o}^r \end{bmatrix} = \mathbf{Z}_k^{e/o} \begin{bmatrix} \mathbf{I}_{e/o}^l \\ \mathbf{I}_{e/o}^r \end{bmatrix} \qquad k = 1, 2, 3 \tag{3}$$

where, $\mathbf{V}$, $\mathbf{I}$ are the amplitude vectors of the transverse components of the E and H-field of the accessible modes, calculated to the left (apex l) and to the right (apex r) of the discontinuity considered. Suffixes e/o stand for even/odd case, respectively.

In the even case, considering TE_{10}, TE_{12}, and TM_{12} as accessible, we get

$$\mathbf{V}_e^s = \begin{bmatrix} V_{e1}^s \\ V_{e2}^s \\ V_{e3}^s \end{bmatrix}, \quad \mathbf{I}_e^s = \begin{bmatrix} I_{e1}^s \\ I_{e2}^s \\ I_{e3}^s \end{bmatrix}, \quad \mathbf{z}_e^{sp} = \begin{bmatrix} z_{e11}^{sp} & z_{e12}^{sp} & z_{e13}^{sp} \\ z_{e21}^{sp} & z_{e22}^{sp} & z_{e23}^{sp} \\ z_{e31}^{sp} & z_{e32}^{sp} & z_{e33}^{sp} \end{bmatrix} \tag{3a}$$

where the indices s, p assume the values l, r.

In the odd case, we take TE_{11}, TM_{11} as accessible, so that each junction reduces to a two-port of the type

$$\mathbf{V}_o^s = \begin{bmatrix} V_{o1}^s \\ V_{o2}^s \end{bmatrix}, \quad \mathbf{I}_o^s = \begin{bmatrix} I_{o1}^s \\ I_{o2}^s \end{bmatrix}, \quad \mathbf{z}_o^{sp} = \begin{bmatrix} z_{o11}^{sp} & z_{o12}^{sp} \\ z_{o21}^{sp} & z_{o22}^{sp} \end{bmatrix}. \tag{3b}$$

Moreover, omitting the suffix e/o, we have in both cases

$$[\mathbf{z}^{sp}]_{ij} = \mathbf{A}_i^{(s)} \cdot \mathbf{Y}^{-1} \cdot \mathbf{A}_j^{(p)} \qquad i, j = 1, 2, 3 \text{ even case } 1, 2 \text{ odd case.} \tag{4}$$

$\mathbf{A}_i^{(l)}$ and $\mathbf{A}_i^{(r)}$ contain the coefficients of the expanding functions used for representing the tangential electric field

of the ith accessible mode at the interface to the left and to the right, respectively, $\mathbf{Y}$ is the discretized Green dyadic admittance.

The latter is obtained by imposing the continuity of the tangential components of the em field at the interface, by following method 3 illustrated in Collin [10], and discretizing the operator so derived by the Ritz–Galerkin method.

The stationarity properties of the impedances $[\mathbf{z}^{sp}]_{ij}$ so obtained are discussed in the same book.

An outline derivation of their expressions and a discussion of the effectiveness of the discretization technique are detailed in the following and in the result section. Here we note just that we use as basis functions for the representation of the tangential electric field at each interface a set of orthonormal polynomials weighted by the correct edge condition. This choice was discussed many times in the past [11]. The main differences with respect to the classical mode expansion can be summarized in the following:

On the one hand, it requires fewer expanding functions to achieve the correct solution and consequently the dimensions of the matrix $\mathbf{Y}$ are smaller; moreover it does not suffer from relative convergence [11]. On the other hand, the computation of the Fourier coefficients and the manipulation of the mode series require more analytical manipulation.

With regard to accuracy obtainable, if the number of expanding functions is adequate in both cases, there are no significant differences between these two choices.

Having computed $\mathbf{Z}_k^e$ and $\mathbf{Z}_k^o$ ($k = 1, 2, 3$) corresponding to the three sub-cases, the behavior of the whole junction is determined by cascading the corresponding transmission matrices $\mathbf{T}_k^e$ and $\mathbf{T}_k^o$.

In fact, denoting by $\mathbf{U}^e(l)$ and $\mathbf{U}^o(l)$ the standard transmission matrices of a waveguide section of length l, for the even/odd excitations, respectively, the global transmission matrix becomes, in the even case

$$\mathbf{T}_E = \mathbf{T}_1^e \cdot \mathbf{U}^e(l_1) \cdot \mathbf{T}_2^e \cdot \mathbf{U}^e(l_2) \cdot \mathbf{T}_3^e \quad : \dim 6 \times 6 \tag{5a}$$

and, in the odd case

$$\mathbf{T}_O = \mathbf{T}_1^o \cdot \mathbf{U}^o(l_1) \cdot \mathbf{T}_2^o \cdot \mathbf{U}^o(l_2) \cdot \mathbf{T}_3^o \quad : \dim 4 \times 4. \tag{5b}$$

When the interaction between junction and filters via modes below-cutoff is negligible, the matrices just obtained can be reduced by closing the ports corresponding to those modes on their characteristic impedances, as illustrated in Fig. 5(a) and (b) for the two excitation cases.

From the latter circuits it is easy to derive the scattering parameters (2a)–(c) and then the response of the diplexer by standard network methods.

III. Computation Effort

In order to retain short computation times the following cares need to be taken.

1) For a given geometry, all Fourier coefficients (7), obtained by the overlapping of modes and expanding functions, are computed once only and stored in an array.

2) The admittance matrix of each discontinuity is obtained in a manner conceptually analogous to [7], that is, by considering

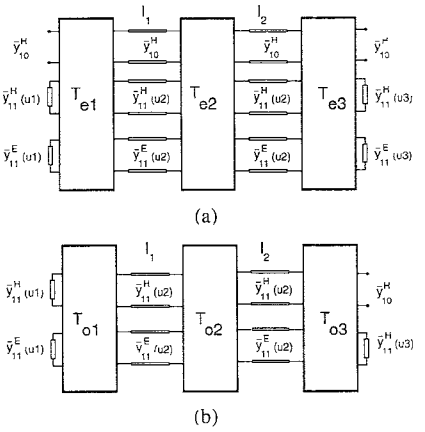

Fig. 5. (a) Equivalent circuit under even excitation at ports 1 and 2: $u1 = b/a$, $u2 = (2b + t)/a$, $u3 = b/a$. (b) Equivalent circuit under odd excitation at ports 1 and 2: $u1 = b/(2a)$, $u2 = (2b + t)/(2a)$, $u3 = b/a$

an appropriate number of accessible modes. Nonetheless, in the present instance the computation is complicated by the different natures of discontinuities 1, 3, and 2, involving the solution of a vector problem. Their exact expressions involve series of the following form, for example, the yy block of the second discontinuity is given by

$$[y_{yy}]_{ij}^{e/o} = \sum_{m=m_l,\, m_l+2} \left[\overline{y}_{m1}^{H}(\overline{b}) + \overline{y}_{m1}^{E}(\overline{b})(\overline{b}m)^2\right] \frac{1}{1+(m\overline{b})^2} \cdot P_{i_y m}(2r) P_{j_y m}(2r) + \sum_{m=m_r,\, m_r+1} \cdot \left[\tilde{y}_{m1}^{He/o}(r)\left(\frac{\overline{b}}{r}\right)^2 + \tilde{y}_{m1}^{Ee/o}(r)\frac{1}{(mr)^2}\right] \cdot \frac{1}{1+[mr/(2\overline{b})]^2} P_{i_y 2m}(1) P_{j_y 2m}(1) \tag{6}$$

where

$$P_{nm}(u) = \sqrt{2u}c_n \frac{J_{1/6+n}\left(\frac{m\pi}{2}u\right)}{\left(\frac{m\pi}{2}u\right)^{1/6}}. \tag{7}$$

These functionals depend on the frequency only via the modal admittances. It is expedient, therefore, to use the exact expressions of the modal admittances just for the first few terms of the above series. Subsequent terms, say past the 10th, can be conveniently approximated. For example, for a modal TE admittance we set

$$\overline{y}_{m1}^{H}(u) = -j\frac{\sqrt{(m/u)^2 - \overline{\omega}^2 - 1 + 1/\overline{b}^2}}{\overline{\omega}} \cong -j\frac{\sqrt{(m/u)^2 - \overline{\omega}_0^2 - 1 + 1/\overline{b}^2}}{\overline{\omega}} \tag{8}$$

where $\overline{\omega}_0$ is the diplexer effective frequency at midband. The modal series containing the previous approximated terms are then computed just once. The latter approximation, in conjunction with the small size of the admittance matrices arising from a prudent choice of the expanding functions, allows extremely short computation times, while maintaining the original accuracy.

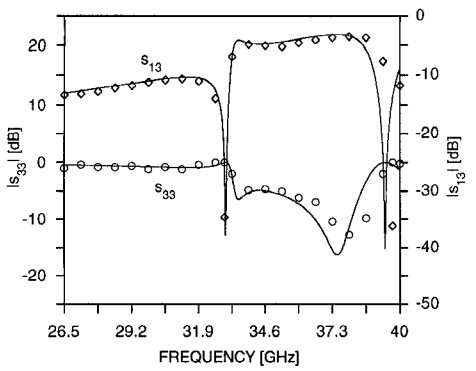

Fig. 6. Comparison between theoretical and experimental scattering parameters of a typical junction. Continuous lines are the theoretical ones, by considering as accessible 5 modes and 7 modes, respectively. Dots are the experimental points.

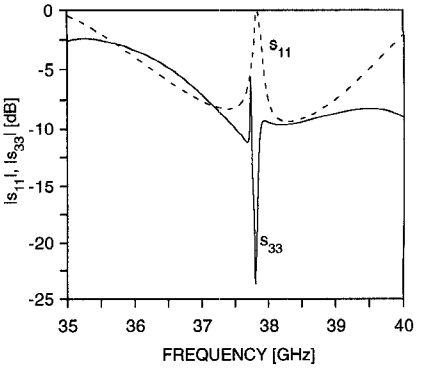

Fig. 7. Reflection magnitudes at ports 1 and 3 of the junction used in the diplexer.

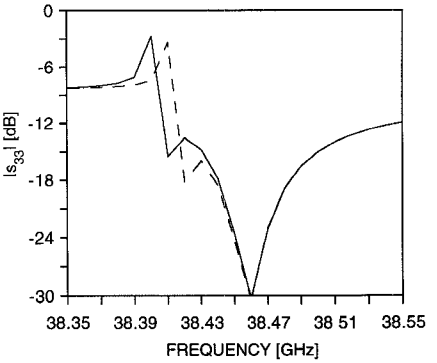

Fig. 8. Comparison between magnitudes of the reflection coefficients at port 1 computed taking account 5 (dashed) and 7 accessible modes (continuous). The junction is the same as that of Fig. 7.

In fact, computing the response of the proposed three-port (5 accessible modes) requires about 6 min on a 486–50 MHz machine, for a full frequency scan (401 points). Computation times increase significantly as more accessible modes are taken into account: for instance, 7 accessible modes require about 11 min.

IV. Results

As a test for the program, Fig. 6 compares experimental and theoretical scattering parameters for a junction of dimensions $a = 7.04$ mm, $b = 3.59$ mm, $t = 1.93$ mm, $d = 0.150$ mm, $s = 0.300$ mm, $l_1 = 1.75$ mm, $l_2 = 4.3$ mm (Fig. 2–3).

It is noted that this is a significant case in as much as the distance between inductive post and bifurcation, l_1, is less than $\lambda_g/4$ at the higher band edge ($\lambda_g = 8.1$ mm at $f = 37$ GHz), implying strong interaction of higher order modes.

The theoretical prediction of the model truncated to 5 accessible modes seems to be in very good agreement with experiment, apart from a slight deviation toward the upper band edge, just where the interaction is strongest. With a view to eliminating this deviation, we increased the number of accessible modes, by including TE_{13} and TM_{13}, but the results were the same as those of the simpler model. Therefore, we concluded that the deviation depends just on mechanical tolerances.

In order to employ the above junction for diplexer applications, its electrical parameters need to be chosen in an appropriate manner. To this end, we adopted the criteria illustrated in [12], briefly stating that over as wide as possible a band, at least over both the bands of the filters, we must have $|s_{11}| = |s_{33}| =$ constant and, preferably, $|s_{11}| \cong 1/3$.

In the case of the following prototypes, it was also required that the characteristics of the two filters were separated by a gap of 1.26 GHz.

The geometry of the junction permitted to approximately satisfy the above requirements just over the two bands of the filters, separated by a region of considerable mismatch, as shown in Fig. 7. This fact did not constitute a limitation in itself, as this region of a mismatch was narrower than the band separating the passbands of the two filters: on the contrary, the isolation between diplexer channels was enhanced. Synthesis, however, was somewhat complicated, by the resonant character of this effect.

Even in this case, we checked the model by increasing the number of accessible modes. As shown in Fig. 8, there is a slight difference just in the resonance region. This constitutes a particularly testing example as small differences between the models of each discontinuity are enhanced by the highly resonant nature of the interposed cavity. In fact, when simulating many nonresonant discontinuities, at even shorter spacings we never encountered deviations comparable with those shown above.

We designed then three diplexers in the band 37–39 GHz by using a single housing with fixed dimensions, tuning only by varying the length of the matching post and its position inside the cavity. This arrangement affords considerable savings in fabrication, as individual diplexers differ only by just an inexpensive mask.

The results obtained, as shown in Fig. 9 for the first diplexer, were satisfactory. Some slight deviations between theoretical and experimental data are due to mechanical tolerances of the filters.

Fig. 10 shows the theoretical response of the lowest of the two 5-poles 26 dB mrl filter employed in the above diplexer. By a comparison with Fig. 9, it can be noted that the diplexer response, designed according the above criteria [12], is seen as transparent by the filters without the need for costly optimization.

Results comparable to those of Fig. 9 are also obtainable from the junction of [2]–[4], but that junction is considerably more expensive than ours. Moreover, it is to be noted that, by suppressing low frequency spurious passbands, selective fre-

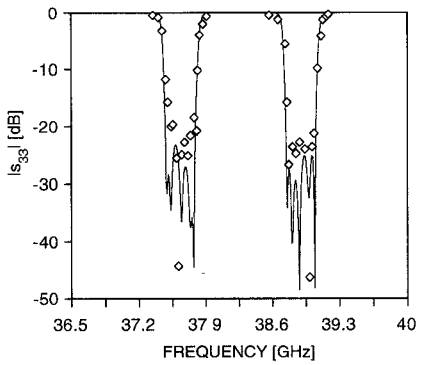

Fig. 9. Comparison between theoretical and experimental (dashed lines) scattering parameters for one of three diplexers realized on the same housing, tuned only by varying position and dimensions of the matching post. Dimensions (in mm) were as follows: Junction: $l_1 = 4.885$, $l_2 = 4.465$, $l_3 = 3.023$, $l_4 = 2.934$, $s = 0.200$, $t = 3.550$. Filters [posts (p), cavities (c)]: filter 1: $p1 = p6 = 1.730$, $c1 = c5 = 7.812$, $p2 = p5 = 5.549$, $c2 = c4 = 7.781$, $p3 = p4 = 6.376$, $c3 = 7.780$; filter 2: $p1 = p6 = 2.026$, $c1 = c5 = 7.301$, $p2 = p5 = 6.422$, $c2 = c4 = 7.259$, $p3 = p4 = 7.360$, $c3 = 7.258$, the thickness of the metallic sheet containing septa is 0.150.

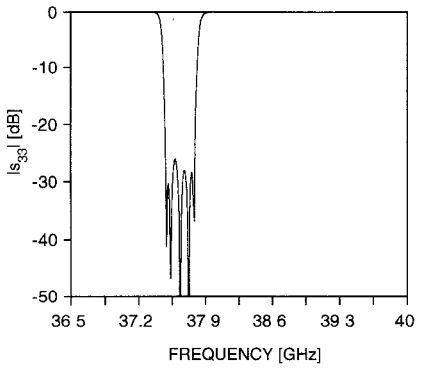

Fig. 10. Theoretical reflection magnitudes of filter 1 employed in the above diplexer.

quency characteristics of the junction allow filters with longer cavities (λ_g, $3/2\lambda_g$) to be employed, which substantially reduce ohmic losses.

Consequently, the arrangement discussed in this work seems to be convenient when the channels are not wide. On the contrary, when specifications require bandwidths wider than 5%, junctions like those of [2]–[4] appear more appropriate.

V. Conclusion

We developed a rigorous analysis for the characterization of a recently proposed "E-plane" diplexer junction of compact and inexpensive fabrication, providing a solution that seems to be expedient when bandwidths are less than 5%.

Different prototypes were built and tested showing good performance, in good agreement with the theoretical predictions.

Appendix
Field Analysis of the Discontinuities

In discretizing the variational expression of the impedances for the three discontinuities under study, we chose polynomials orthonormal over the appropriate intervals as expanding functions. The weight functions take into account the inverse cubic root singularity of the normal electric field in proximity of the 90°-metal corners. By means of integration by parts, the nonsingular component of the electric field was also transformed into a singular function satisfying the same boundary and edge conditions as the normal E-field [11]. In all cases, complete convergence was obtained with just three expanding functions for each field component.

With reference to the coordinate system of Fig. 2, the following expansions were employed.

For discontinuities of the type 1 and 3

$$\frac{b\varepsilon_o}{2\pi}\frac{dE_x}{dy}(x,y) = 2\sqrt{\frac{1}{ab\varepsilon_o}}\cos\frac{\pi}{a}x\sum_{k=1,2}^{3} X_k^{(i)} W \cdot [\eta^{(i)}(y)] f_{\mu(k)}[\eta^{(i)}(y)] \tag{A1a}$$

$$E_y(x,y) = 2\sqrt{\frac{\varepsilon_o}{ab}}\sin\frac{\pi}{a}x\sum_{k=1,2}^{3} Y_k^{(i)} W[\eta^{(i)}(y)] \cdot f_{\nu(k)}[\eta^{(i)}(y)] \tag{A1b}$$

discontinuity 1, even case

$$\mu(k) = 2k,$$
$$\nu(k) = 2(k-1),$$
$$\varepsilon_o = 1,$$
$$\eta^{(1)}(y) = \frac{2y}{b}$$

discontinuity 1, odd case

$$\mu(k) = 2k-1,$$
$$\nu(k) = 2k-1,$$
$$\varepsilon_o = 1$$

discontinuity 3, even case

$$\mu(k) = 2k,$$
$$\nu(k) = 2(k-1),$$
$$\varepsilon_o = 2,$$
$$\eta^{(3)}(y) = \frac{b+t/2-y}{b}$$

discontinuity 3, odd case

$$\mu(k) = 2k,$$
$$\nu(k) = 2(k-1),.$$
$$\varepsilon_o = 2$$

For discontinuities of the type 2

$$E_x(x,y) = \frac{2}{\sqrt{b}}\sqrt{\frac{2}{a-d}}S_x^{e/o}(y)\sum_{k=1,2}^{3} X_k^{(2)} \cdot W\left[\frac{2x}{a-d}\right] f_{\mu(k)}\left[\frac{2x}{a-d}\right] \tag{A2a}$$

$$\frac{dE_y}{dx}(x,y) = \frac{1}{\sqrt{b}}\sqrt{\frac{2}{a-d}}S_{y1}^{e/o}(y)\sum_{k=1,2}^{3} Y_k^{(o)} \cdot W\left[\frac{2x}{a-d}\right] f_{\mu(k)}\left[\frac{2x}{a-d}\right] \tag{3b}$$

$$+\frac{2}{\sqrt{b}}\sqrt{\frac{2}{a-d}}\,S_{y2}^{e/o}(y)\sum_{k=1,2}^{3}Y_k^{(2)}\cdot W\left[\frac{2x}{a-d}\right]f_{\mu(k)}\left[\frac{2x}{a-d}\right] \tag{A2b}$$

where d is the post thickness, $\mu(k)=2k$; discontinuity 2, even case

$$S_x^e(y)=\sin\frac{\pi}{b+\frac{t}{2}}y,$$
$$S_{y1}^e(y)=1,$$
$$S_{y2}^e(y)=\cos\frac{\pi}{b+\frac{t}{2}}y \tag{A3a}$$

discontinuity 2, odd case

$$S_x^o(y)=\cos\frac{\pi}{2\left(b+\frac{t}{2}\right)}y,$$
$$S_{y1}^o(y)=0,$$
$$S_{y2}^o(y)=\sin\frac{\pi}{2\left(b+\frac{t}{2}\right)}y \tag{A3b}$$

$$N_x=N_y=3$$
$$f_k(t)=\frac{1}{N_k}G_k^{1/6}(t) \tag{A4a}$$
$$W(t)=(1-t^2)^{-1/3}. \tag{A4b}$$

Where $G_k^{1/6}(t)$ is the kth Gegenbauer polynomial of order 1/6 and the constant N_k was chosen as to satisfy the following orthonormality conditions [13]

$$\int_0^1 dt\,W(t)G_n^{1/6}(t)G_m^{1/6}(t)=N_m^2\delta_{nm} \tag{A4c}$$

$$N_m=\frac{2^{-1/6}}{\Gamma\left(\frac{1}{6}\right)}\left[\frac{\pi\Gamma\left(\frac{1}{3}+m\right)}{\left(\frac{1}{6}+m\right)m!}\right]^{1/2} \tag{A4d}$$

ACKNOWLEDGMENT

The authors are indebted to Dr. Gulloch, Dr. Politi, Mr. Brambilla, Mr. Cereda, and Dr. Bianconi of Alcatel-Telettra, Vimercate Italy, for providing experiments and for helpful discussions.

REFERENCES

[1] Y. Shih, L. Q. Bui, and T. Itoh, "Millimeter-wave diplexers with printed circuit elements," *IEEE Trans. Microwave Theory Tech.*, vol. MTT-33, no. 12, pp. 1465–1469, Dec. 1985.

[2] J. Dittloff and F. Arndt, "Rigorous design of septate multiplexers with printed circuit elements," in *IEEE MTT-S Dig.*, 1988, pp. 431–434.

[3] ——, "Rigorous field theory design of millimeter-wave E-plane integrated circuit multiplexers," *IEEE Trans. Microwave Theory Tech.*, vol. MTT-37, no. 2, pp. 340–350, Feb. 1989.

[4] R. Vahldieck and B. Varailhon de la Filolie, "Computer aided design of parallel-connected millimeter-wave diplexers/multiplexers," in *IEEE MTT-S Dig.*, 1988, pp. 435–438.

[5] H. Yao, A. Abdelmonem, J. Liang, X. Liang, K. Zaki, and A. Martin, "Wide-band waveguide and ridge waveguide T-junction for diplexer applications," *IEEE Trans. Microwave Theory Tech.*, vol. 41, no. 12, pp. 2166–2173, Dec. 1993.

[6] A. Morini, T. Rozzi, D. De Angelis, and W. Gulloch, "A novel matched diplexer configuration in E-plane technology," *IEEE MTT-S Dig.*, 1993, pp. 1077–1080.

[7] T. Rozzi, F. Moglie, A. Morini, W. Gulloch, and M. Politi, "Accurate full-band equivalent circuits of inductive posts in rectangular waveguide," *IEEE Trans. Microwave Theory Tech.*, vol. 40, no. 5, May 1992.

[8] R. R. Mansour and R. Macphie, "An improved transmission matrix formulation of cascaded discontinuities and its application to E-plane circuit," *IEEE Trans. Microwave Theory Tech.*, vol. MTT-34, no. 12, Dec. 1986.

[9] T. Rozzi, "Network analysis of strongly coupled transverse apertures in wave-guides," *Int. J. Circuit Theory Applicat.*, vol. 1, pp. 161–178, June 1973.

[10] R. E. Collin, *Field Theory of Guided Waves*, 2nd ed. Piscataway, NJ: IEEE Press, 1990.

[11] F. Alessandri, M. Mongiardo, T. Rozzi, G. Schiavon, and R. Sorrentino, "Alcuni nuovi aspetti sulla convergenza delle tecniche di raccordo modale in strutture guidanti a microonde," in *Proc. VIII RINEM*, 1990, pp. 143–146.

[12] A. Morini and T. Rozzi, "Design of 'optimum' three port symmetrical junctions for diplexer application," in *IEEE MTT-S Dig.*, 1994, pp. 739–742.

[13] S. Gradshtein and I. M. Rhyzik, *Table of Integrals Series and Products*. New York: Academic, 1965.

Antonio Morini (M'94) was born in Italy in 1962. He received the degree in electronic engineering (summa cum laude) from the University of Ancona in 1987 and the Ph.D. degree in electromagnetism in 1992.

Since 1992, he has been with the Department of Electronics and Automatics at the University of Ancona as an Assistant Professor. His current research interests are modeling and synthesis of passive millimetric components, such as filters, multiplexers, and antennas.

Tullio Rozzi (M'66–SM–74–F'90) received the dottore degree in physics from the University of Pisa in 1965, and the Ph.D. degree in electronic engineering from Leeds University in 1968. In June 1987, he received the D.Sc. degree from the University of Bath, Bath, UK.

From 1968–1978, he was a Research Scientist at the Philips Research Laboratories, Eindhoven, the Netherlands, having spent one year, 1975, at the Antenna Laboratory, University of Illinois, Urbana. In 1978, he was appointed to the Chair of Electrical Engineering at the University of Liverpool and was subsequently appointed to the Chair of Electronics and Head of the Electronics Group at the University of Bath, in 1981, where he also held the responsibility of Head of the School of Electrical Engineering on an alternate three-year basis. Since 1988, Dr. Rozzi has been Professor of Antennas in the Department of Electronics and Control, University of Ancona, Italy, while remaining a Visiting Professor at Bath University.

Dr. Rozzi was awarded the Microwave Prize by the IEEE Microwave Theory and Technique Society, in 1975. He is also a Fellow of the IEE (UK) as well as IEE Council Representative for Italy.